

BANG-BANG

DIELECTROPHORETIC ORIENTATION

by

James R. Melcher, David S. Guttman
and Mathew Hurwitz

CSR-TR-68-1

January, 1968

BANG-BANG DIELECTROPHORETIC ORIENTATION

James R. Melcher^{*} and David S. Guttman[†]

Massachusetts Institute of Technology
Cambridge, Mass.

and Mathew Hurwitz^{††}

Dynatech Corporation, Cambridge, Mass.

The Korteweg-Helmholtz force density on a homogeneous incompressible dielectric liquid immersed in an electric field is concentrated at interfaces. Hence, an electric field imposed with a strong gradient in the region of an interface has a marked effect on the fluid dynamics. As the interface passes from a field-free region through the gradient, the electric surface force "bangs" on. Experiments are described which demonstrate the influence of the electric field on modes of fluid oscillation. It is demonstrated that liquids such as freon and nitrogen can be suspended in a stable equilibrium over a gas in an adverse, "one g" gravitational field. Experimental measurements of oscillation frequency and conditions for instability are correlated with a theoretical model which includes the salient non-linear features of the dynamics. Applications to slosh control and orientation of liquids in low gravity environments are discussed.

* Associate Professor of Electrical Engineering, Member, AIAA

† Teaching Assistant, Dept. of Electrical Engineering

†† Manager, Advanced Systems Department, Member AIAA

Nomenclature

C = capacitance of analogue experiment

d = plate thickness

\overline{E} = electric field intensity

E_o = rms or dc electric field intensity between plane, parallel
electrodes

$F = (\epsilon - \epsilon_o) E_o^2 / 2ol$

\overline{F} = force density

f = frequency of oscillation (Hz/sec)

f_o = frequency of oscillation with no electric field

g = gravitational acceleration

l = length of equivalent fluid pendulum

p = hydrostatic pressure

s = electrode spacing

T = period of oscillation

T_e = surface force density

T_1 = 1/4 of time slosh spends in bang-bang region

T_2 = 1/4 of time slosh spends in linear region

t = time

U = total potential energy

U_e = potential energy due to electric field intensity

U_g = potential energy due to gravity

\overline{v} = fluid velocity

$\gamma = 2\xi_m/s$ - slosh peak amplitude normalized to plate spacing

ϵ = permittivity of liquid

ϵ_o = permittivity of free space

(Nomenclature continued)

$\epsilon(x,y,z,t)$	=	permittivity, a function of position x,y,z and time
λ	=	characteristic wavelength on interface
η	=	$E_0 \sqrt{(\epsilon - \epsilon_0)/2\rho g s}$
ξ	=	displacement of equivalent fluid pendulum
ξ_m	=	maximum average amplitude of slosh, and maximum deflection of equivalent pendulum
ξ_p	=	deflection at which potential has maximum value with g "adverse"
ρ	=	mass density of liquid
τ_e	=	total electric force per unit area acting on fluid pendulum
τ_g	=	gravity force per unit area acting on fluid pendulum
τ_{max}	=	maximum force per unit area on pendulum
ω_0	=	angular slosh frequency with no electric field

Background

For some time it has been recognized that the storage of cryogenics for long-duration space missions may require some means for controlling the position of the liquid and vapor.¹ There are many classes of propellant control problems which must be dealt with: one, for example, is the suppression of slosh growth upon a sudden change or cut-off of engine thrust.² This paper will show that electrohydrodynamic systems, which have been under serious development since 1961 as a means for propellant orientation,^{3,4,5} can also provide a significant influence on the dynamics of a sloshing surface. The non-linear, bang-bang stabilization phenomenon discussed here can be considered as an extreme case of the field gradient stabilization developed previously.⁶ It not only provides an engineering solution to a class of orientation problems, but makes possible meaningful tests in liquid-vapor systems (such as those involving cryogenics) in an earth-bound laboratory environment.

In the design of dielectrophoretic liquid storage systems, it is natural to think in terms of replacing the effect of gravity with that of the electric field. Instead of the force density ρg , the electric field intensity \bar{E} induces the force density

$$\bar{F} = \epsilon \nabla \left(\frac{1}{2} E^2 \right) \quad (1)$$

where ϵ is the liquid permittivity.

Although the force density written as Eq. (1) has the most obvious analogy to that due to gravity, it obscures the fundamental fact that the effect of the electric field on the incompressible fluid motions is completely

determined by the fields at the free interface. This is true because forces which are purely the gradient of a pressure do not affect the incompressible dynamics of the liquid, and if the force density $-\nabla \frac{1}{2} \epsilon E^2$ is added to Eq. (1), the resulting dynamics will be unaltered, but the force density becomes^{7,8}

$$\bar{F} = -\frac{1}{2} E^2 \nabla \epsilon \quad (2)$$

In this form, it is clear that the electric polarization force density influences the liquid at the interface where ϵ undergoes an abrupt change, and therefore $\nabla \epsilon$ is not zero, as it is in the bulk. In some cases it is fruitful to think in terms of an analogy between dielectrophoretic forces and surface tension forces because, in a homogeneous liquid, the electric field produces only a surface force.

The "gravity-like" representation of Eq. (1) suggests that, to orient or control a liquid, the volume of interest should be filled with an electric field having as nearly as possible a constant E^2 gradient. By contrast, Eq. (2) suggests that the $\text{grad } E^2$ field could be confined to the region of the interface, since that is the only region where it will have any influence. Of course, if the interface can be anywhere in the tank initially, the two viewpoints do not differ. Thus, where total dielectrophoretic orientation is required, the field gradient stabilization approach⁶ would be adopted.*

There are classes of space missions, however, where slosh control or partial propellant orientation are required under conditions such that, at

* A review of related work concerned with dielectrophoretic orientation is given in reference 6.

critical times the interface position is essentially known. For example, a propellant tank may be accelerated into orbit with a programmed sequence of events. Then, as in the S-IV-B when the propulsion engines are shut down and low gravity conditions are established (by the ullage thrusters), the interface position is known. In such a situation it would be appropriate to design an electrohydrodynamic slosh baffle with fields confined to the region of the interface. This not only has the advantage of allowing for use of electrodes over a restricted volume of the total tank, but as will be shown here, makes possible the use of a greatly enhanced "bang-bang" interaction with the fluid.

A significant consequence of the bang-bang interaction is that liquids can be oriented against gases in the laboratory using this mechanism, with the attendant advantage of being able to conduct earth-bound experiments under conditions that are conservative compared to those expected in space. In the past, it has been necessary to simulate liquid cryogenics oriented against their vapors (for example) by using liquid-liquid systems. Because of the many differences in the electromechanical properties of these two two-phase systems, it has not been possible until now to obtain information on such important factors as the reliability of dc fields. In liquid-liquid systems, the dc fields often produce instability,^{9,10} and as will be discussed in the following sections, the bang-bang orientation mechanism has made it possible to study the effect of dc fields in orienting liquid-vapor systems in the laboratory against adverse normal accelerations.

Bang-Bang Electrohydrodynamics

It follows from Eq. (2) that an interface between a liquid and its vapor is subject to the surface force density

$$T_e = \frac{1}{2} (\epsilon - \epsilon_0) E^2 \quad (3)$$

in a direction normal to the surface acting from the liquid to the vapor.

Figure 1 shows the electrode arrangement that can be used to suppress the amplitude of slosh. In this example, g is taken as acting in a direction that is favorable to the orientation (positive g), as would be the case, for example, at engine cut-off when the S-IV-B vehicle is injected into orbit. Sloshing occurs with the equilibrium position of the interface essentially coincident with the upper edges of the electrodes. These electrodes alternately have opposite potentials, so that between adjacent electrodes having the spacing s , there is an essentially uniform electric field intensity E_0 , independent of whether or not the liquid occupies that region.

As the liquid sloshes in the mode shown in Fig. 1, the interface on one side leaves the field region between the plates, while on the other side it enters the field region. At the instant shown in Fig. 1, the interface at (a) is essentially out of the fringing field and free of any electric surface force, while that at (b) experiences the surface force given by Eq. (3). Note that this surface force tends to return the interface to the equilibrium position, and is constant so long as the depressed interface at (b) is between the electrodes. For surface displacements large compared to the plate spacing s , the interface experiences an electric surface force $(\epsilon - \epsilon_0) E_0^2 / 2$ that either "bangs" full on, and tends to return it to equilibrium, or "bangs" full off.

The bang-bang interaction is at the opposite extreme from the case considered in reference 6, in that gradients in E^2 are distributed over an interval of surface deflections which is small, rather than large, compared

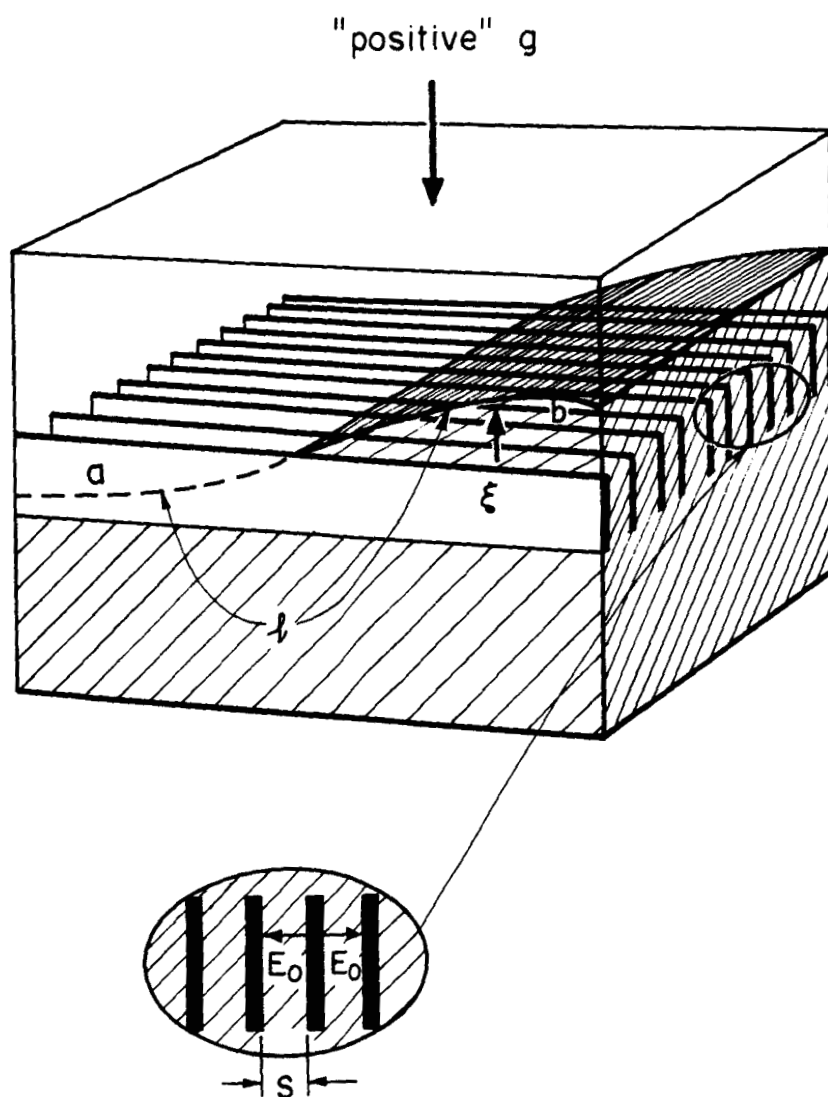


Fig. 1 Example of a dielectrophoretic slosh baffle that takes advantage of the bang-bang effect.

to possible excursions of interest.

The slosh suppression of Fig. 1 illustrates the first of two aspects of this problem to be considered. The second is illustrated by Fig. 2, where it is incidental that the electrodes take on a coaxial rather than parallel plate configuration. The important point is that g acts adversely, or so as to disorient the liquid, and in addition to the question of slosh dynamics, there is the question of stability.

The Theoretical Model

The bang-bang interaction is inherently non-linear, and an exact analysis of the fluid motions would not only be extremely complex, but of little use in the engineering design of an orientation system. In reference 6 it was shown that a simple pendulum model for the liquid system gave a surprisingly complete picture of the essential dynamics. It will be found that this is the case here as well.

The pendulum model for the bang-bang interaction is shown in Fig. 3, where ξ is an equivalent average of the slosh amplitude and l is the length of an equivalent pendulum which would have the same natural frequency as the system of Fig. 1, say, in the absence of the electric field. The length l would of course be different for different tank geometries and for different modes of slosh.¹¹

The equilibrium plane of the interface (the upper edge of each plane, parallel electrode) is at $x = 0$. Although the pendulum model of Fig. 3 shows only interfaces between two pairs of parallel electrodes, it is important to keep in view the fact that interfacial displacements of interest have characteristic wavelengths λ in the plane of the interface

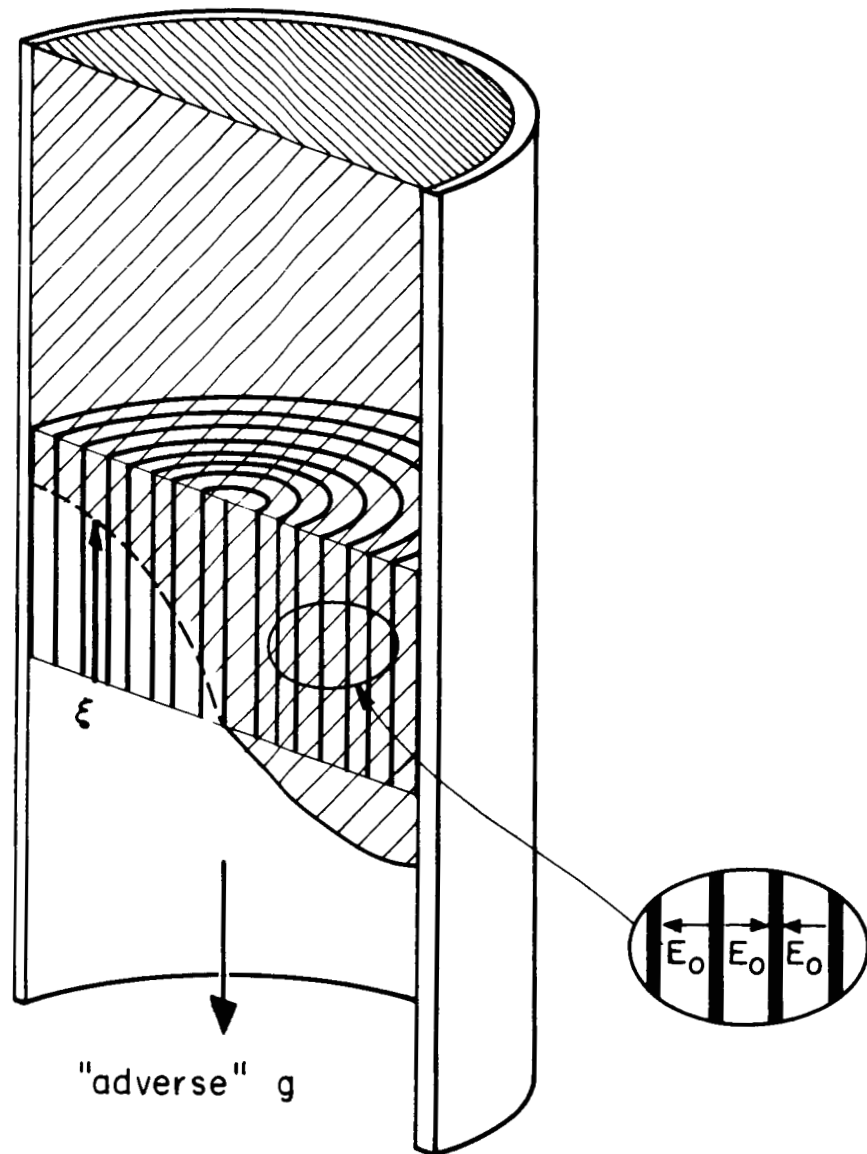


Fig. 2 Example of bang-bang orientation in the face of an adverse acceleration g

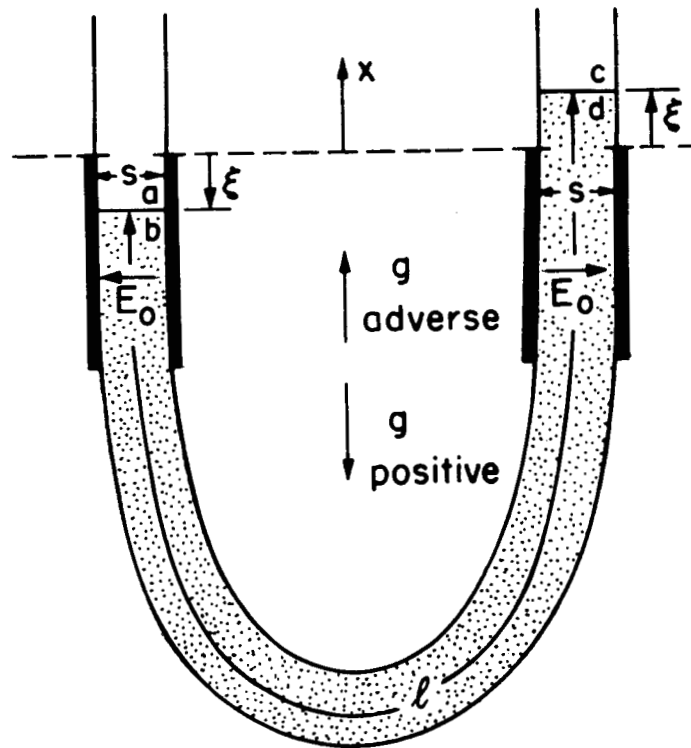


Fig. 3 Pendulum model for situations of Figs. 1 and 2. The deflection ξ and length l are "equivalent" averages for the actual modes.

that are long compared to the interelectrode spacing, s . (The liquids wet the electrodes.) The effects of the electric field on the dynamics are determined by the degree to which the electric surface traction is altered as the liquid is displaced. There are two contributions to this change, one from the change in imposed electric field at the interface due to its change in position, and the second from the change in the electric field brought about by the surface deformation itself. It can be shown that these latter "self-field" effects are ignorable if:

$$\left| \frac{\epsilon - \epsilon_0}{\epsilon + \epsilon_0} \right| \left(\frac{s}{\lambda} \right) \ll 1 \quad (4)$$

In the dynamics of interest here, either slosh suppression or stability, it is the longest wavelengths that are the most dangerous, hence this approximation is justified. Furthermore, because $\lambda \gg s$, it is appropriate to ignore the detailed nature of the fringing field at the upper edges of the electrodes.

According to Eq. (2), there is no electric force in the bulk of the liquid, and so long as attention is confined to the bulk, the usual dynamic form of Bernoulli's equation is applicable.

$$\int_b^d \frac{\partial}{\partial t} \rho \vec{v} \cdot d\vec{\ell} + \left[p + \rho g x + \frac{1}{2} \rho v^2 \right]_b^d = 0 \quad (5)$$

The limits of integration through the liquids are just below the interfaces, as shown in Fig. 3. The first term is approximated by the product of a pendulum length ℓ and the velocity $\partial \xi / \partial t$, and Eq. (5) becomes:

$$\rho \ell \frac{d^2 \xi}{dt^2} = \tau_g + p_b - p_d \quad (6)$$

where $\tau_g = -\partial U_g / \partial \xi$ with $U_g = \rho g \xi^2$ in the case where g is positive. The same procedure shows that the pressures at a and c just above the interfaces are equal, because the gas in the upper region is of negligible density. (Note that if the force density of Eq. (1) is used, this is not true.) For convenience, p_a and p_c are taken as zero, so that p_d and p_b are respectively, the negatives of the electrical surface forces acting upward on the right and left interfaces, as given by Eq. (3). These subtract to give the total surface force $\tau_e = -p_d + p_b$ shown in Fig. 4 as a function of ξ .

The dependence on ξ of the total electrical surface force acting on the pendulum has been divided into two parts. There is a linear range $-\frac{s}{2} < \xi < \frac{s}{2}$ where the interface is still in the fringing fields, and

$$\tau_e = -(\epsilon - \epsilon_0) E_0^2 \xi / s \quad (7)$$

$$U_e = -\frac{1}{2} (\epsilon - \epsilon_0) E_0^2 s \left(\frac{\xi}{s} \right)^2 \quad (8)$$

where U_e is a potential function defined such that $\tau_e = -\partial U_e / \partial \xi$.

Beyond the linear region, there is the bang-bang region $|\xi| > \frac{s}{2}$ where

$$\tau_e = -(\epsilon - \epsilon_0) E_0^2 / 2 \quad (9)$$

$$U_e = (\epsilon - \epsilon_0) E_0^2 s \left(\frac{\xi}{2s} - \frac{1}{8} \right) \quad (10)$$

The extent of the linear region assumed here is determined by capacitance measurements as described in the appendix.

Slosh Dynamics

The piecewise continuous potential U_e , as well as U_g with g positive and the total potential $U = U_e + U_g$ are sketched in Fig. 4b. This simple

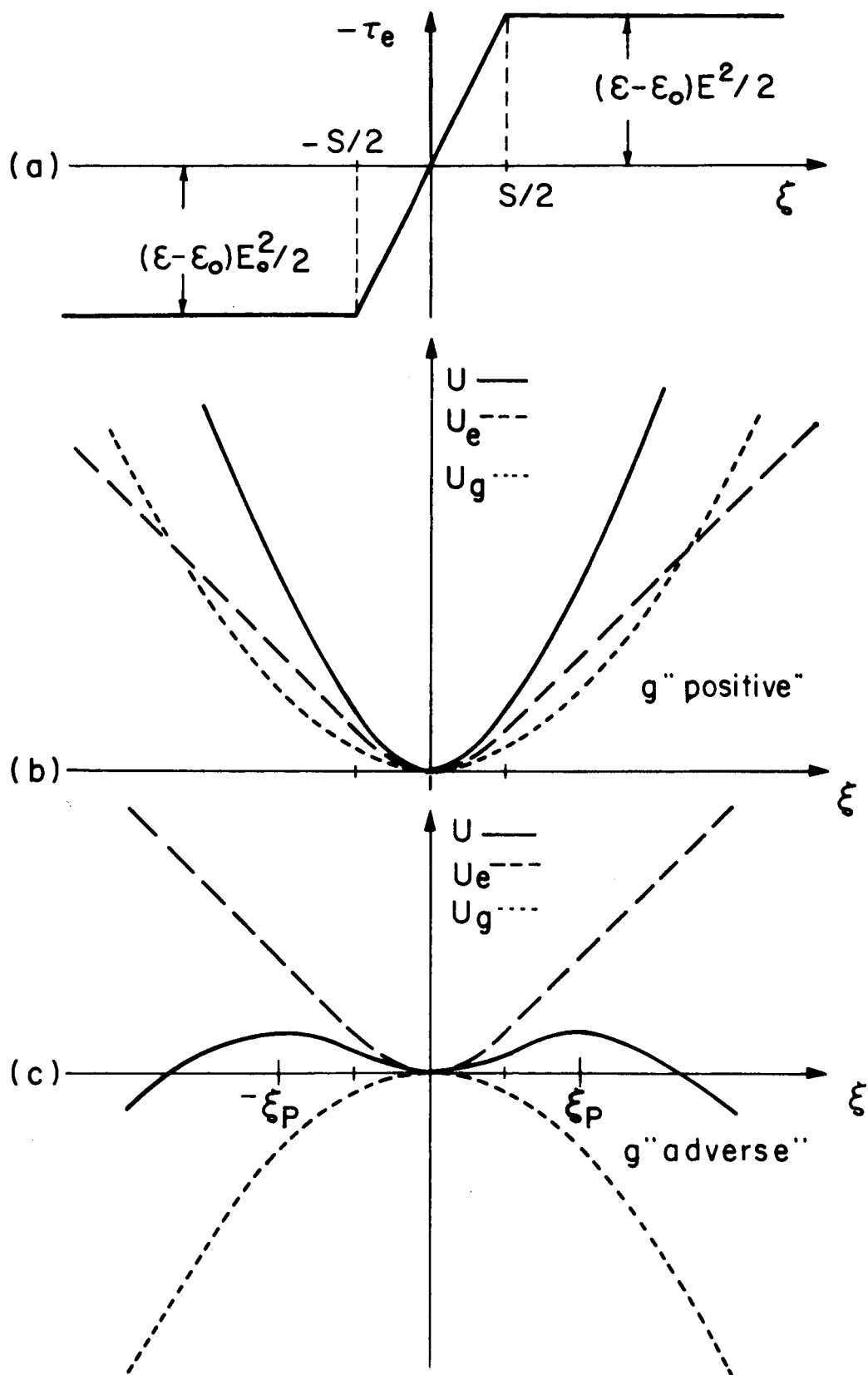


Fig. 4

a) Total electrical surface force acting on pendulum of Fig. 3.

b) Electric, gravitational, and total potential for positive acceleration

c) as in (b), but with g adverse

model makes it possible to relate the peak slosh amplitude ξ_m to the parameters of the electrohydrodynamic baffle and hydrodynamic system. In the linear range, the pendulum equation becomes

$$\frac{d^2\xi}{dt^2} + \omega_o^2 \left(1 + \frac{2F}{s\omega_o^2} \right) \xi = 0 \quad (11)$$

where

$$F = (\epsilon - \epsilon_o) E_o^2 / 2\rho l \text{ and } \omega_o^2 = 2g/l$$

while in the bang-bang range

$$\frac{d^2\xi}{dt^2} + \omega_o^2 \xi = -F \quad (12)$$

From Eq. (11) it follows that, so long as the peak amplitude ξ_m is less than $s/2$, the slosh frequency is

$$\frac{f}{f_o} = \sqrt{1 + \eta^2} \quad (13)$$

where $f_o = \omega_o/2\pi$ and $\eta = E_o \sqrt{(\epsilon - \epsilon_o)/2\rho g s}$

To determine the slosh frequency when the peak deflection is in the bang-bang range, T_1 and T_2 are respectively defined as $1/4$ of the times required for the fluid pendulum to traverse the bang-bang and linear regions as it executes one cycle. Thus the period of oscillation is:

$$T = 4 (T_1 + T_2) \quad (14)$$

To compute T_1 , assume that $\xi = \xi_m$ when $t = 0$. By definition of ξ_m ,

$\frac{d\xi}{dt}(0) = 0$ and from Eq. (12),

$$\xi = \left(\xi_m + \frac{F}{\omega_o^2} \right) \cos \omega_o t - \frac{F}{\omega_o^2} \quad (15)$$

Then, since $\xi = s/2$ when $t = T_1$, it follows that

$$\omega_o T_1 = \cos^{-1} [(\eta^2 + 1)/(\gamma + \eta^2)] \quad (16)$$

where $\gamma = 2\xi_m/s$

To compute T_2 , Eq. (11) is solved, given that when $t = 0$, $\xi = s/2$ and $d\xi/dt$ has the value given by Eq. (15) when $t = T_1$ (the time origin is shifted by T_1)

$$\xi = -\left(\xi_m + \frac{F}{\omega_o^2}\right) \frac{\sin \omega_o T_1}{\sqrt{1 + \eta^2}} \sin \omega_o \sqrt{1 + \eta^2} t + \frac{s}{2} \cos \omega_o \sqrt{1 + \eta^2} t \quad (17)$$

Then, when $t = T_2$, $\xi = 0$ and T_2 must satisfy the equation:

$$\frac{-(\gamma + \eta^2)}{\sqrt{1 + \eta^2}} \sin \omega_o T_1 \sin \omega_o \sqrt{1 + \eta^2} T_2 + \cos \omega_o \sqrt{1 + \eta^2} T_2 = 0 \quad (18)$$

Finally, Eq. (16) is used to eliminate T_1 from Eq. (18) and an expression is obtained for T_2

$$\omega_o T_2 = \frac{1}{\sqrt{1 + \eta^2}} \tan^{-1} \left\{ (1 + \eta^2) / [(\gamma + \eta^2)^2 - (\eta^2 + 1)^2] \right\}^{\frac{1}{2}} \quad (19)$$

Given the normalized electric field intensity η and normalized slosh amplitude γ , Eqs. (16) and (19) provide $\omega_o T_2$ and $\omega_o T_1$, which in turn determine the slosh frequency f normalized to the frequency in the absence of the electric field.

$$\frac{f}{f_o} = \pi/2 (\omega_o T_1 + \omega_o T_2) \quad (20)$$

The slosh frequency is shown in Fig. 5. Note that, according to the piece-wise continuous potential model, Eq. (20) is valid for $\gamma > 1$. For $\gamma < 1$, f/f_0 is found from Eq. (13) and is independent of γ , as shown in Fig. 5.

Stability

Stability is of major interest when the bang-bang concept is applied to orientation systems assuming the configuration illustrated in Fig. 2. Here, the fluid is in an unstable equilibrium in the absence of the electric field, a situation equivalent to subjecting the pendulum model of Fig. 3 to an adverse acceleration g , as shown. Thus, g in Eqs. (11) and (12) is replaced by $-g$, and the potentials have the dependence on ξ sketched in Fig. 4c.

For a peak excursion ξ_m that does not exceed $s/2$, the point of incipient instability follows from Eq. (11) ($g \rightarrow -g$) as:

$$\eta = \eta^* = 1 ; \quad \gamma < 1 \quad (21)$$

where again $\eta = E_0 \sqrt{(\epsilon - \epsilon_0)/2\rho g s}$ and η^* is the critical normalized E_0 . That is, if the normalized electric field intensity does not exceed unity, even infinitesimal oscillations are unstable.

If, for the adverse g case, the amplitude of the excursion ξ_m exceeds $s/2$ ($\gamma > 1$), the equilibrium is unstable for amplitudes ξ_m that exceed the deflection ξ_p as shown in Fig. 4c. Note, ξ_p is the deflection where the the potential reaches its maximum value. Thus, in the bang-bang range of peak slosh amplitudes, the equilibrium is stable if

$$\eta < \eta^* = \sqrt{\gamma} \quad (22)$$

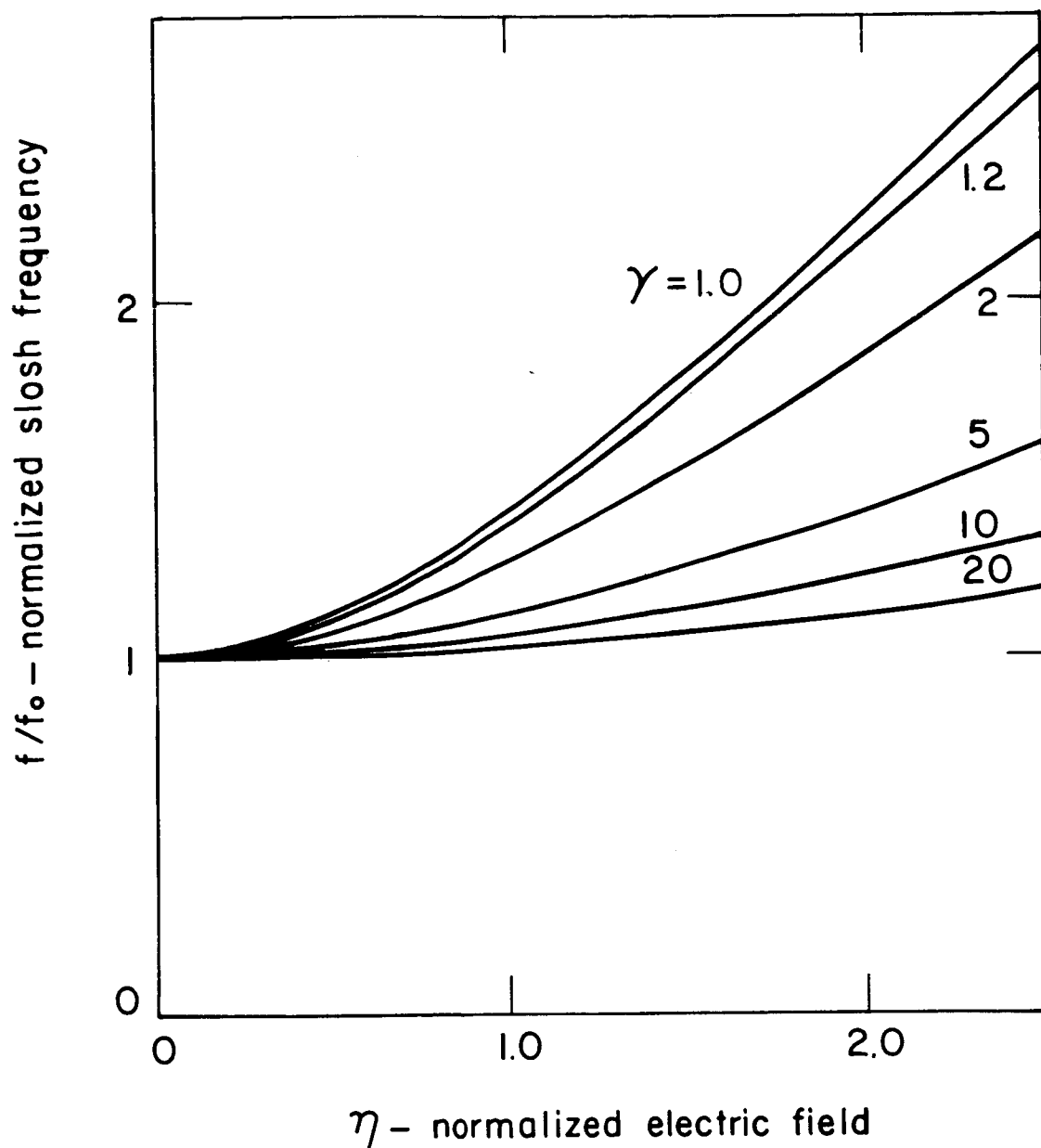


Fig. 5 Slosh frequency f normalized to frequency f_0 in the absence of electric field as a function of the normalized electric field intensity. γ is the slosh amplitude normalized to half of the interelectrode spacing.

The stability regimes, as a function of the normalized slosh amplitude, are summarized in Fig. 6. As might be expected on physical grounds, a greater electric field is required to stabilize the larger slosh amplitudes. Of course, the piecewise continuous marginal stability curve is a consequence of the piecewise continuous potential model. In actuality, it would be expected that the curve would be smooth in the region of transition near $\gamma = 1$.

Experiments: AC Fields

It is difficult to obtain experimental conditions wherein the polarization force density of Eq. (2) is not dominated by free charge effects. Fields of alternating polarity, having a frequency much greater than the reciprocal relaxation time, can be used to avoid effects from free charges that accrue in the fluid through relaxation (conduction) phenomena. In the experiments to be described in this section, the electric field had a frequency of 400 Hz., a value considerably in excess of that required to avoid relaxation effects in the fluids used. A relatively high frequency was used because with 60 Hz. fields, the response of a liquid-gas interface to the 120 Hz. component of the force was significant, as evidenced by short wavelength vibrations of the interface. This dynamic response, characterized by a frequency twice that of the imposed ac fields, is not of interest here. Hence, the 400 Hz. fields were used both to avoid the relaxation effects and to eliminate fluid interactions involving the second harmonic of the imposed fields. In computing the electrical force, the ac field is considered as a dc field having the same rms value.

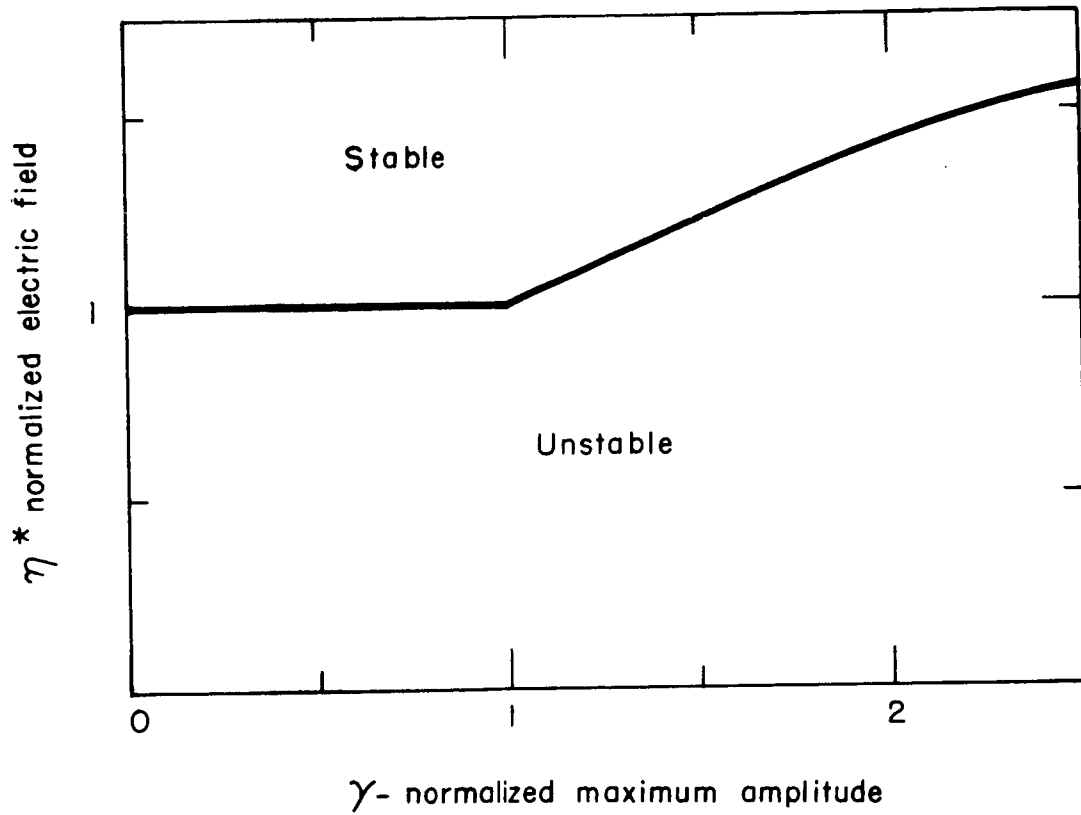


Fig. 6 Critical normalized electric field intensity for stable slosh, as a function of the maximum amplitude normalized to the half interplate spacing

Two classes of experiment are of interest: the first concerned with slosh modes in a positive g , and the second stability in an adverse g , as exemplified by the situations of Figs. 1 and 2. Measurements of the slosh dynamics were obtained from a plexiglas tank of rectangular cross-section (7.5 x 12.5 cm) having the electrode geometry of Fig. 1. The electrodes were 1/8 inch thick brass plates with a 2.2 cm. vertical height and 0.38 cm. spacing.

The objective of the slosh experiments was to see if the simple predictions summarized in Fig. 5 are meaningful in an engineering context. Thus, measurements were made of the lowest slosh mode resonance frequency (the natural frequency predicted by the potential well mode) as a function of applied electric field and slosh amplitude.

In the dynamic experiments it was essential to retain a relatively high Q for the resonance in spite of the damping effect of the electrodes. Hence, a low viscosity fluid, Freon 113, was used and horizontal vibrations of the tank in the direction of the electrodes were used to excite the mode shown in Fig. 7a. In this picture, the fluid is seen at its peak amplitude, essentially as sketched in Fig. 1, with no applied electric field. The effect of applying 14 kv between the plates is evident in Fig. 7b, where all other conditions of Fig. 7a are retained and the picture was taken with the amplitude peaking to the left. The original slosh amplitude is almost completely attenuated.

If the frequency of excitation is raised, keeping the applied field and excitation the same, the slosh amplitude is returned to its original value, although somewhat revised in shape, as shown in Fig. 7c. Thus, the electric field had a stiffening effect on the interface that was on

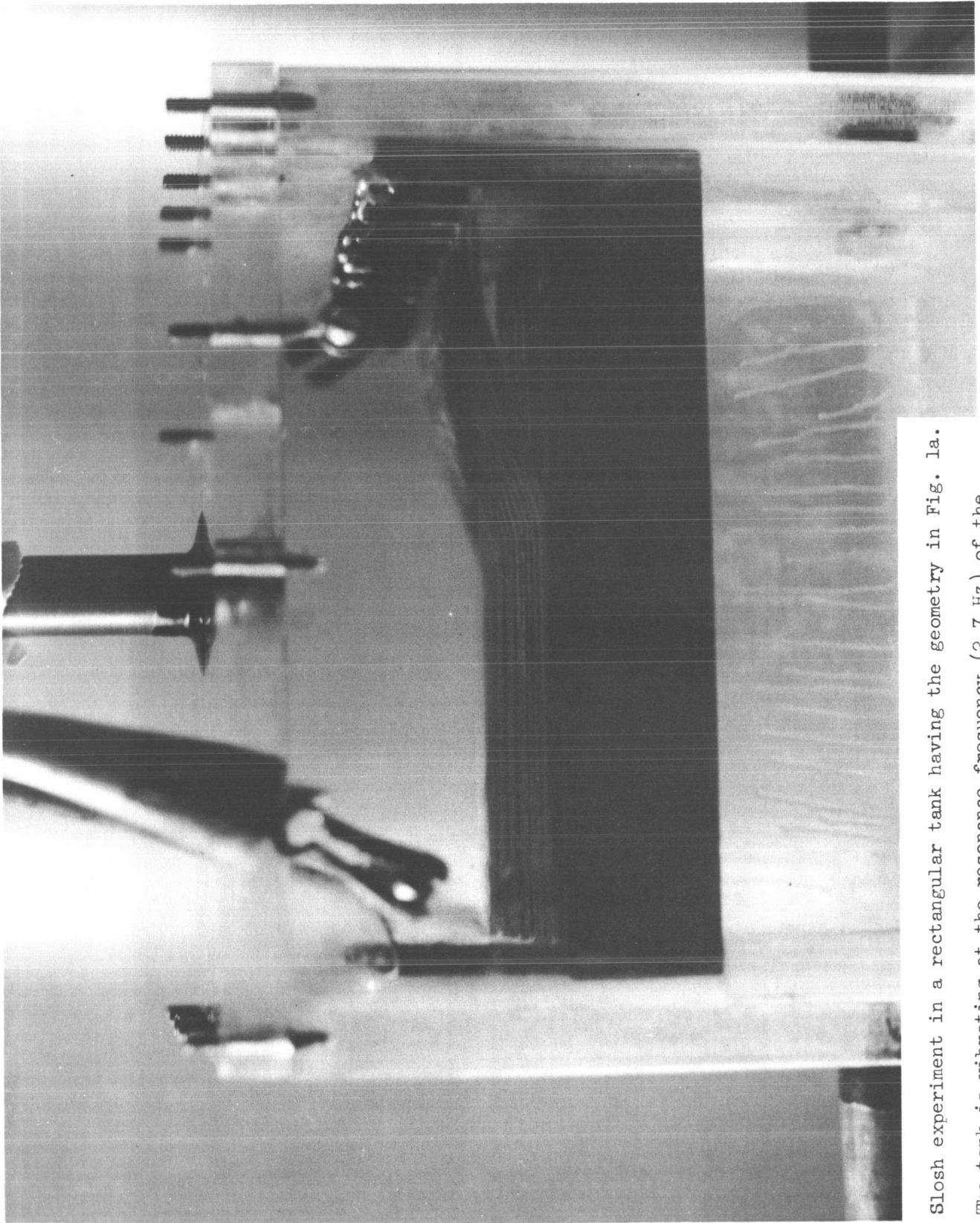


Fig. 7a Slosh experiment in a rectangular tank having the geometry in Fig. 1a. The tank is vibrating at the resonance frequency (2.7 Hz) of the lowest sloshing mode with no voltage.

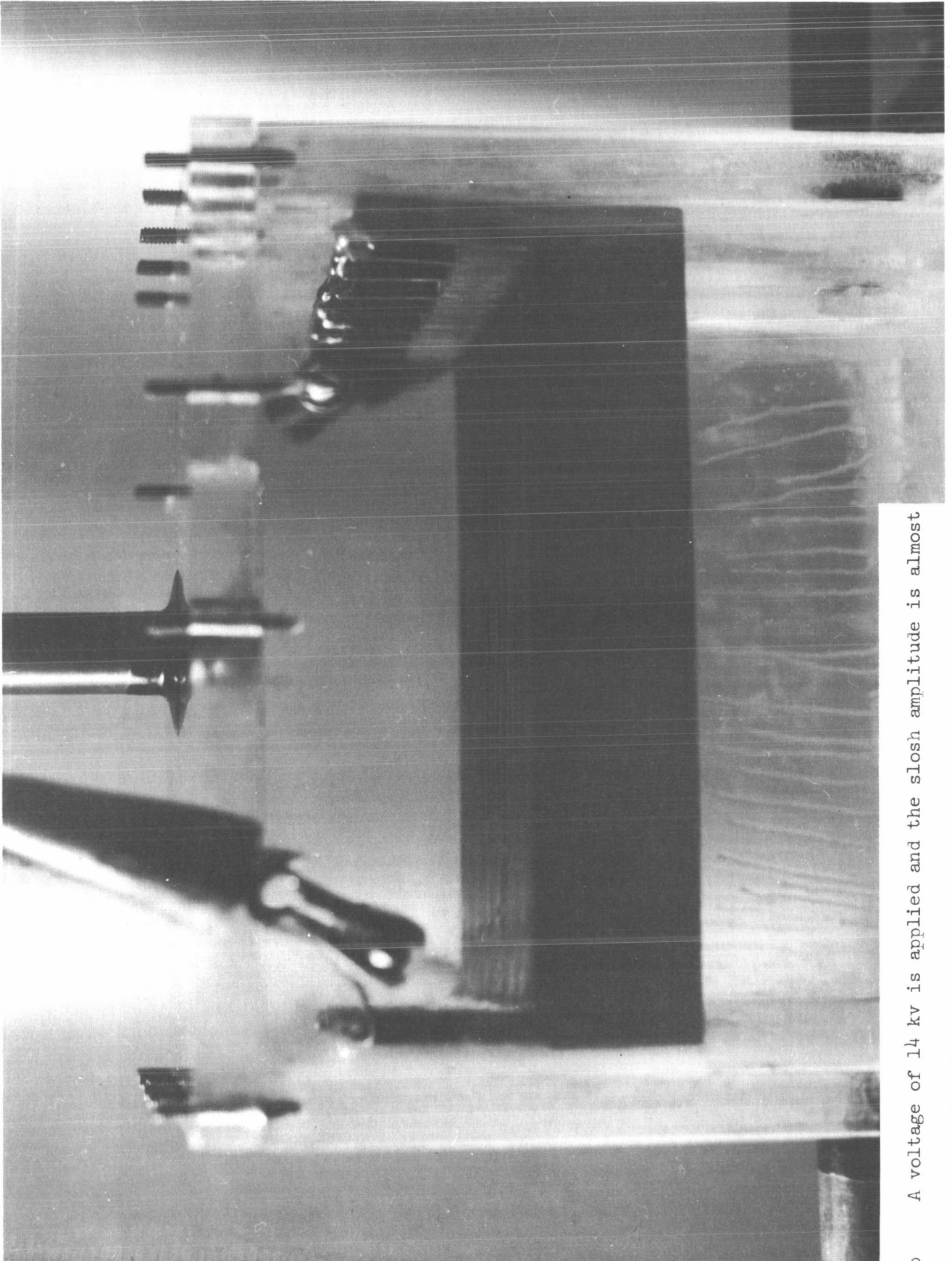


Fig. 7b A voltage of 14 kv is applied and the slosh amplitude is almost completely attenuated.

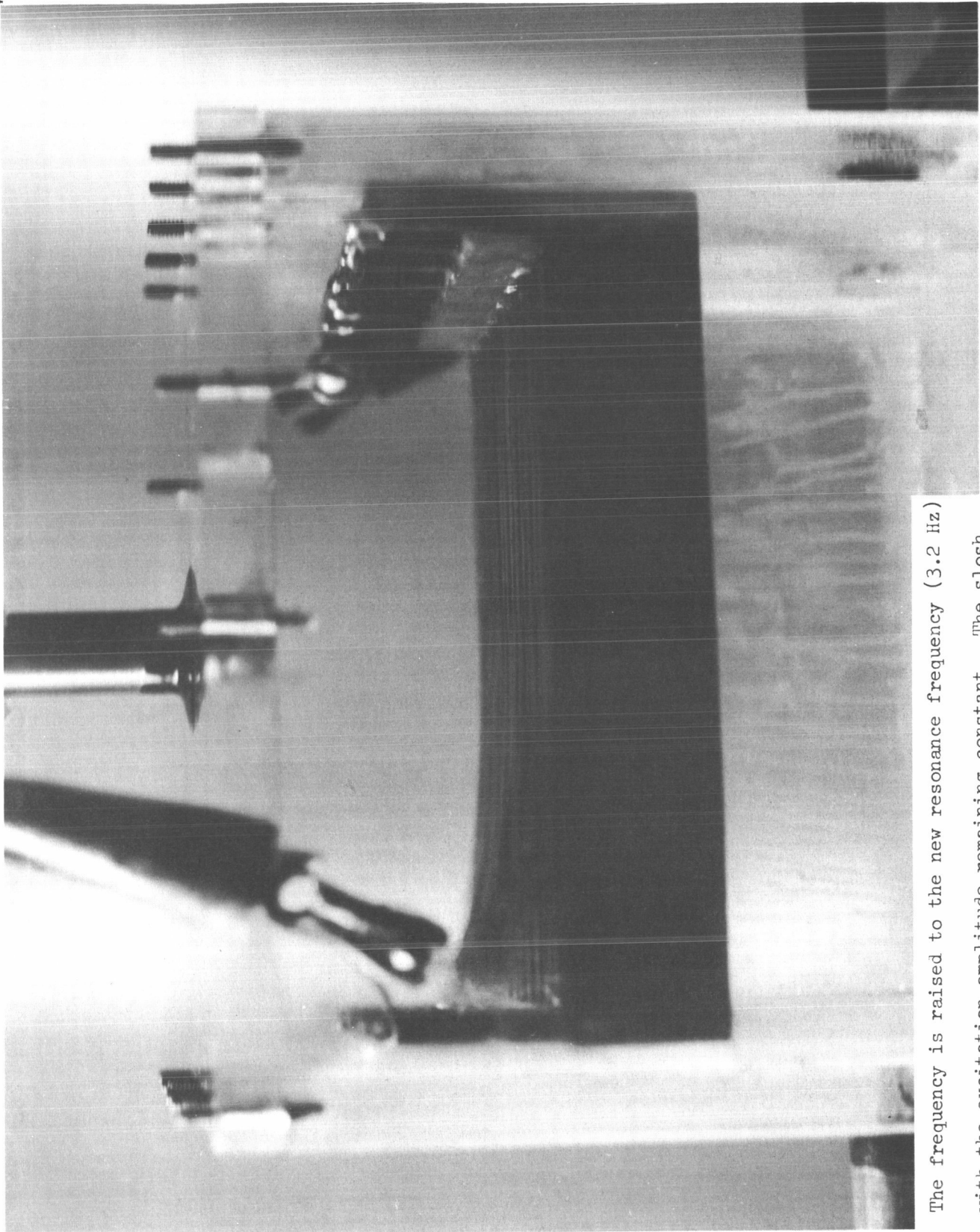


Fig. 7c

The frequency is raised to the new resonance frequency (3.2 Hz)

with the excitation amplitude remaining constant. The slosh

amplitude takes on a somewhat different appearance, but has essentially the same amplitude as in Fig. 7a.

the same order as that produced by a normal (one g) gravitational acceleration. It is important to recognize that the frequency shift, rather than the slosh attenuation at a given frequency, is the meaningful measure of the degree to which the field prevents slosh amplification in a space application as g is suddenly reduced.

The discrete pendulum model, of course, can describe only the average of the interface motions. Even so, the simple model gives a remarkably quantitative prediction of the dynamics. It is reasonable to define peak deflection of the equivalent pendulum as $1/\sqrt{2}$ that of the slosh amplitude. The measured frequency shifts for small and large amplitude slosh are compared to the predictions in Fig. 8. Note that $\gamma = 3.5$ corresponds to a peak amplitude that is still less than the vertical height of the electrodes.

The pendulum model ignores the continuum nature of the bang-bang interaction. Thus, it does not account for changes in the slosh mode shape, even as observed over the limited range of variables in a one g experiment (compare Figs. 7a and 7c). Although, in the experiments discussed here, the effects of gravity and the electric field were clearly demonstrated to be on the same order, there were no situations in which the effect of gravity was ignorable compared to that of the electric field. It must be recognized that in the low gravity condition, the predictions of the simple pendulum model might not be in as close agreement with experiment as is indicated by Fig. 8. This is true because the continuum aspects of the bang-bang dynamics would then be dominant in determining the spatial distribution of the interface deflections.

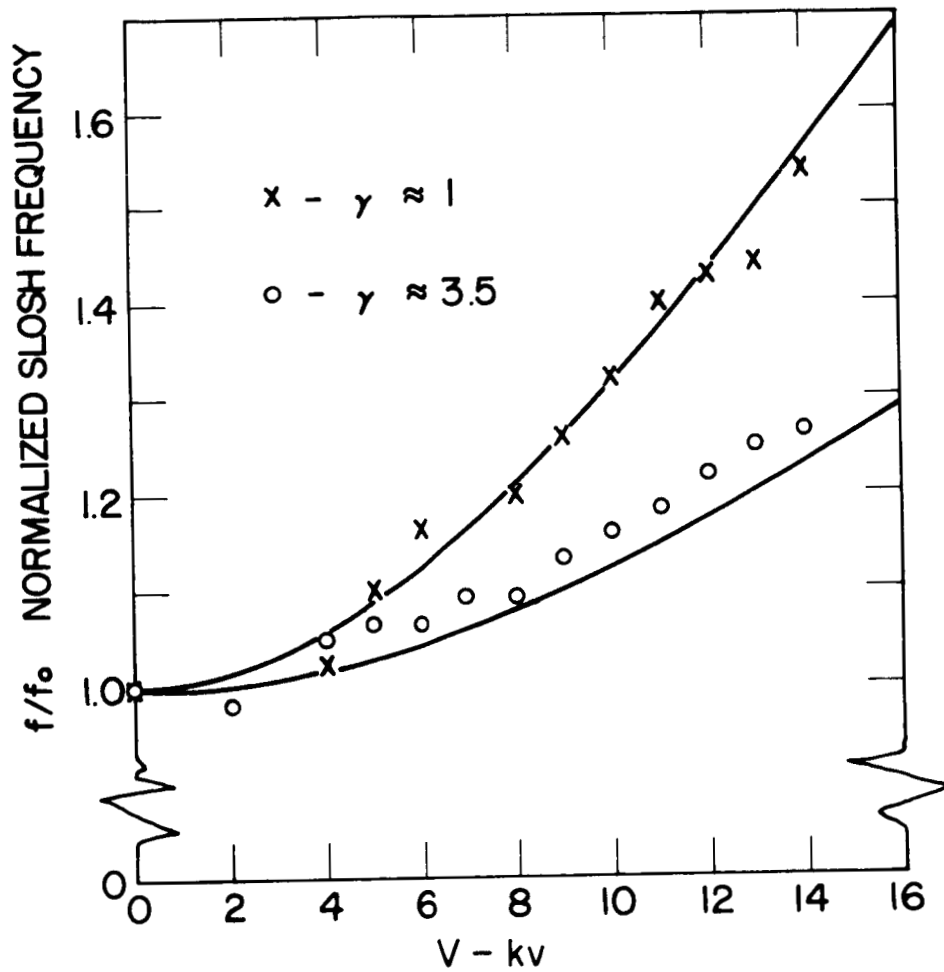


Fig. 8 Experimentally observed frequency shift as a function of voltage for the experiment of Fig. 7. The fluid is Freon 113. The solid curves are given by the theoretical model and the correlation clearly shows the effect of the amplitude.

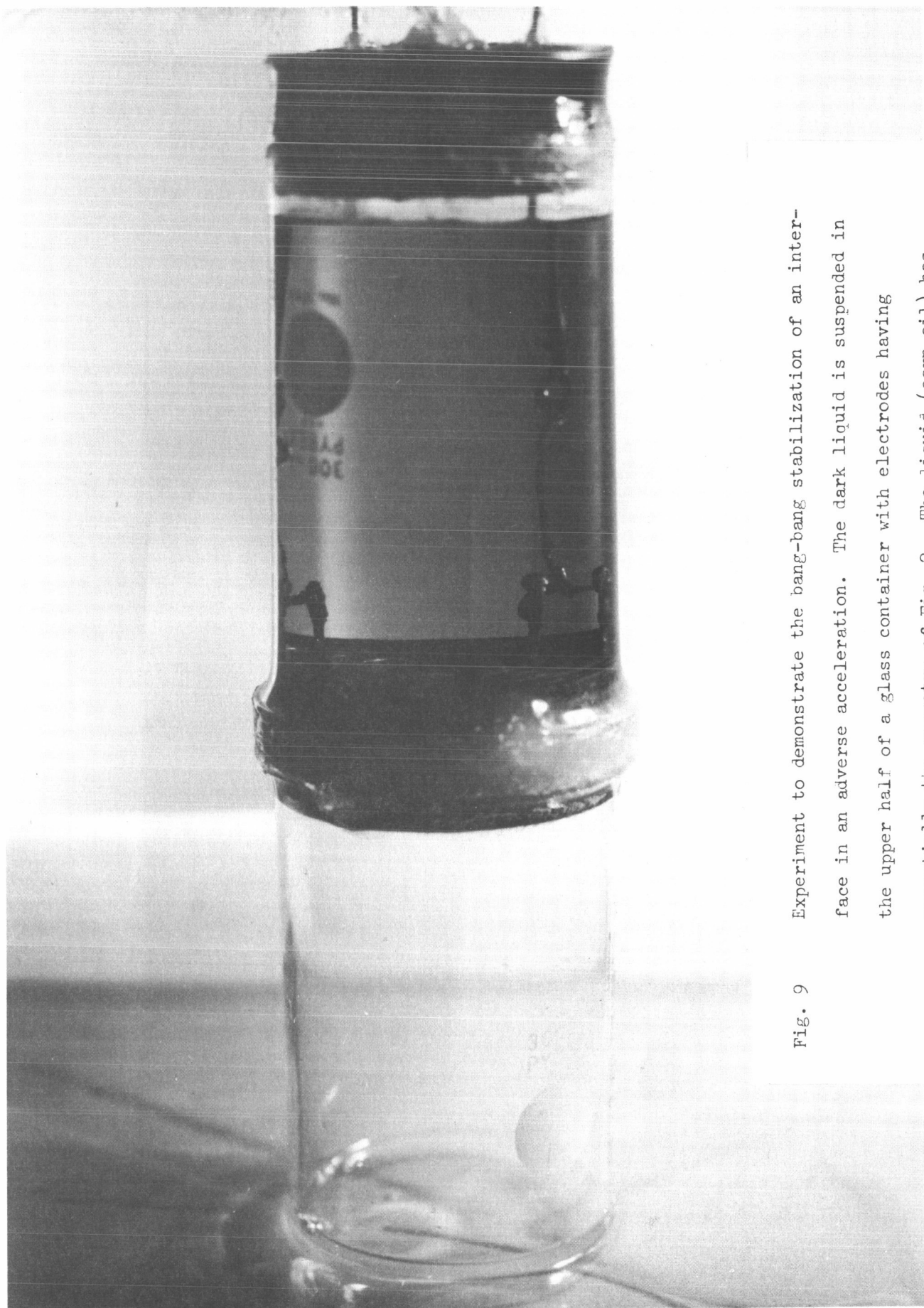


Fig. 9 Experiment to demonstrate the bang-bang stabilization of an interface in an adverse acceleration. The dark liquid is suspended in the upper half of a glass container with electrodes having essentially the geometry of Fig. 2. The liquid (corn oil) has been removed from the bottom half of the cylinder.

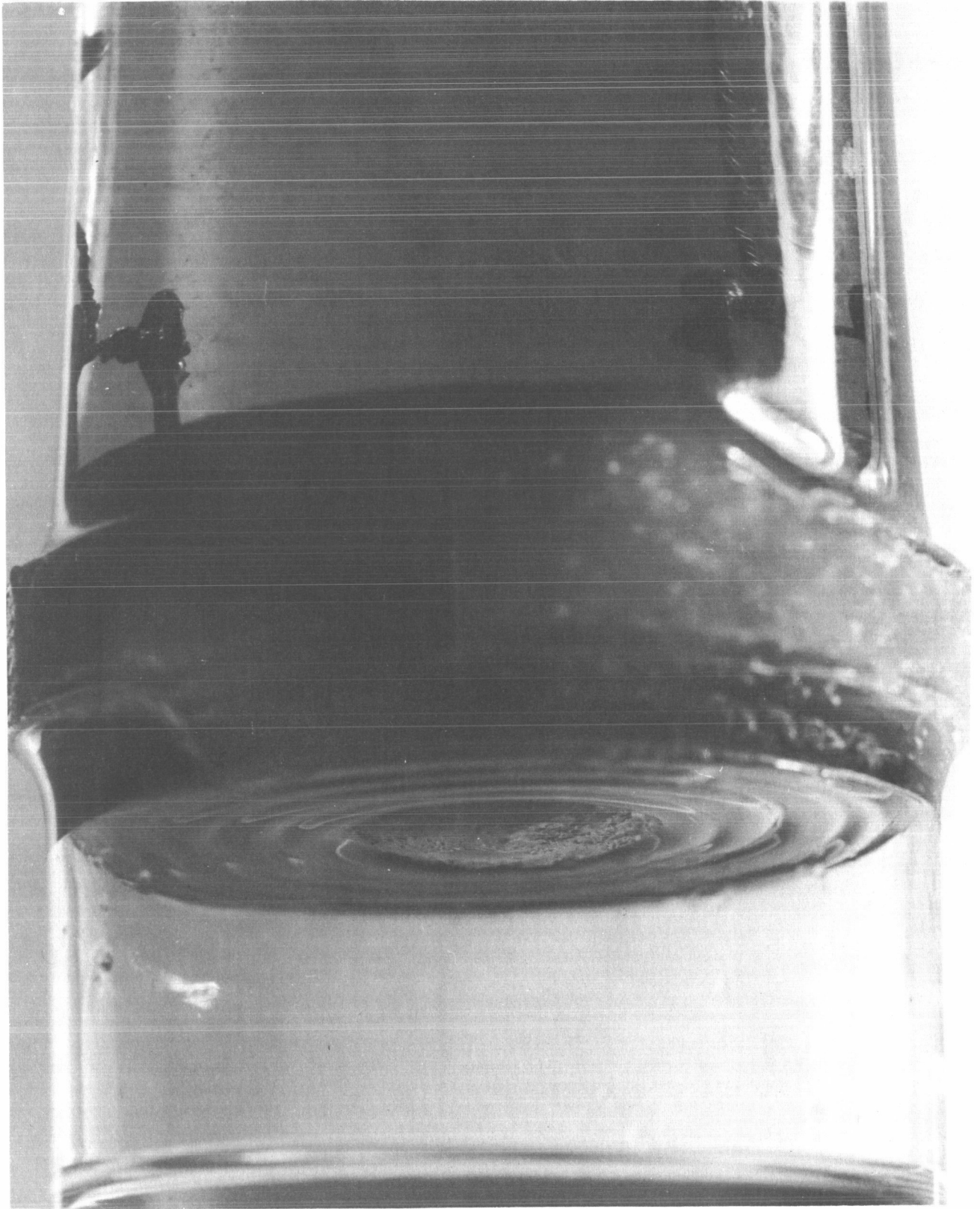


Fig. 10 Closeup view of lower edges of electrodes and fluid interface for the experiment of Fig. 9.

Fig. 10a Voltage above that required to maintain stable interface with small amplitude deflections.



Fig. 10b Instability resulting from a reduction in voltage below that required for stability. Note that the interface to the right has risen, while that to the left is falling.

A second class of ac experiments had the objective of investigating the stability predictions of Eq. (21) in an adverse acceleration. The configuration sketched in Fig. 2 is shown experimentally in Fig. 9. A glass cylinder of circular cross-section, 6 cm. inside diameter, was separated into two sections by coaxial electrodes (interelectrode spacing $s = 0.32$ cm.). The top of the cylinder was closed off by a rubber stopper and the bottom placed in a pan of dielectric liquid (in the picture, corn oil). Thus, with the voltage off the liquid could be sucked into the cylinder so that both the regions above and below the electrodes were filled. Then the voltage was applied to the electrodes and the liquid allowed to drain from the lower section of the cylinder by bubbling Freon gas into the lower section, to avoid breakdown. Because of the bang-bang stabilization of the interface at the lower edges of the electrodes, the bubbles were stopped at the electrodes when the field was applied, and the liquid remained in the upper part of the cylinder as shown in Fig. 9. (where the corn oil was dyed for photographic purposes). A closeup view of the stabilized interface is shown in Fig. 10a, where it can be seen that the electrodes were wetted by the fluid. When the voltage was reduced below a critical value, the configuration was unstable, and the liquid fell from the upper section of the cylinder. The view of Fig. 10b was taken shortly after incipience of instability. If the field was reapplied, after the fluid began to fall through the electrodes, the motion could be stopped and the interface returned to stable equilibrium. The electric field has the effect of a valve between the upper and lower sections of the cylinder.

It is important to distinguish between stabilizing the interface and supporting a column of liquid. The idea that the electric field supports the column of liquid deserves careful consideration in any case, since the force density of Eq. (2) is downward. The hydrostatic pressure in a liquid

must always be taken into account in determining the static equilibrium. Even if the electric field did act in a direction to support the liquid column, the maximum force would be only sufficient to support a column 0.65 cm. high under the experimental conditions. Yet, a column 10 cm. high was supported indefinitely. The basic limitation here on the height of the column is one of vapor pressure, not of electric pressure. The electric field simply stabilizes the interface.

A quantitative comparison between experimental conditions for incipient instability with infinitesimal slosh amplitude and the predictions of the pendulum model is made in Fig. 11. The solid line, which is predicted by Eq. (21), gives a reasonable estimate of the conditions for instability. Experimental errors arise because of variations in the way in which the liquid wets the electrodes and the glass walls of the container. Most of the liquids tended to wet both. Pertinent fluid parameters are summarized in Table 1.

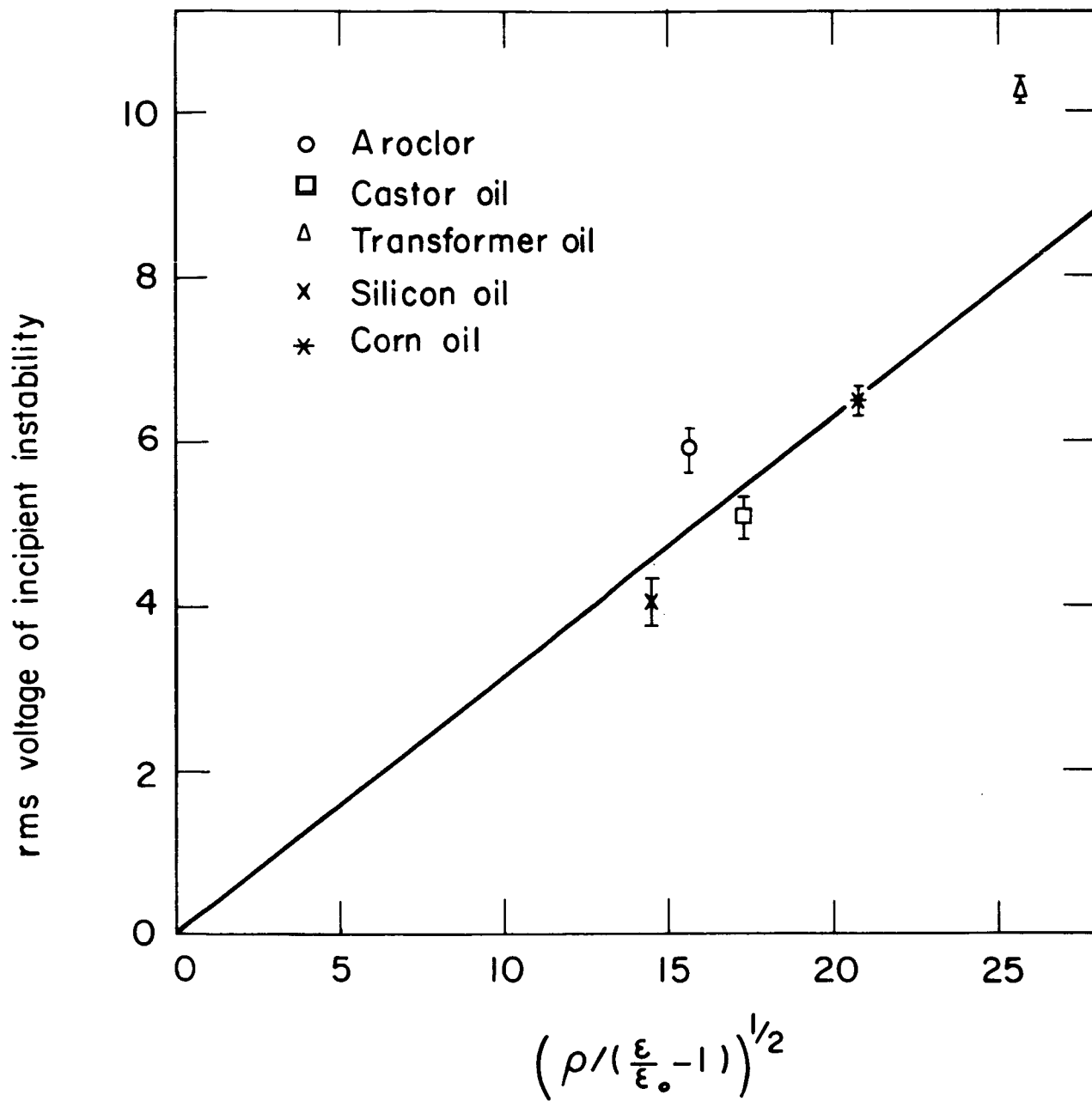


Fig. 11 Voltage for incipient instability in experiment of Figs. 9 and 10 as function of pertinent fluid parameters. The solid line is the theory, Eq. (21).

Table 1. Data for Fluids Used in Incipient Instability Experiments

<u>Fluid</u>	<u>Relative Permittivity ϵ/ϵ_0</u>	<u>Density (Units of 10^3 kg/m^3)</u>
Aroclor 1232 (Monsanto)	5.7	1.14
Castor Oil (Howe & French)	4.7	1.1
Transformer Oil (GE 10-C)	2.2	0.8
Silicon Oil (Dow Corning 1265)	6.95	1.25
Corn Oil (Mazola)	3.1	0.91
Freon 113	2.41	1.56
Liquid Nitrogen	1.43	0.8

Experiments: DC Fields

There are three effects that generally account for differences between results, such as those just described, where ac fields are used and where dc fields are used. In the dc fields, the fluids are prone to forms of instability related to the relaxation of free charge, while the electrical breakdown strength of the dielectric can tend to be degraded by the accumulation of space charge due to emission effects at the electrodes.¹⁰ On the other hand, interfacial vibration and instability induced by the pulsating nature of the ac field-induced forces is not present with the dc fields. In the ac experiments this difficulty was avoided by using a sufficiently high-frequency electric field.

Experiments have been conducted in essentially the same configuration as previously described, but with dc fields. For the cases tested (fluids with relaxation times exceeding 10^{-2} seconds) it was found that the voltage for incipient instability with ac and dc fields differed by less than 15%. Of greatest significance were stability experiments conducted using liquid nitrogen with dc fields. The experimental configuration was essentially as described in the previous section, with provision made for maintaining the cryogenic environment as shown in Fig. 12. The apparatus consisted of a glass tube with a set of concentric cylindrical electrodes carefully fitted to prevent leakage between the outer electrode and the cylinder. The glass tube with its electrode array was positioned in an unsilvered glass dewar and suspended from a fiberglass cover as shown in Fig. 12. The experiment began by drawing liquid nitrogen into the glass tube using a vacuum pump. When the tube was nearly full, the tube vent was sealed off and the electric field was established by connecting the electrode array to a filtered source of dc high voltage. Following this, nitrogen gas was bubbled beneath the electrodes

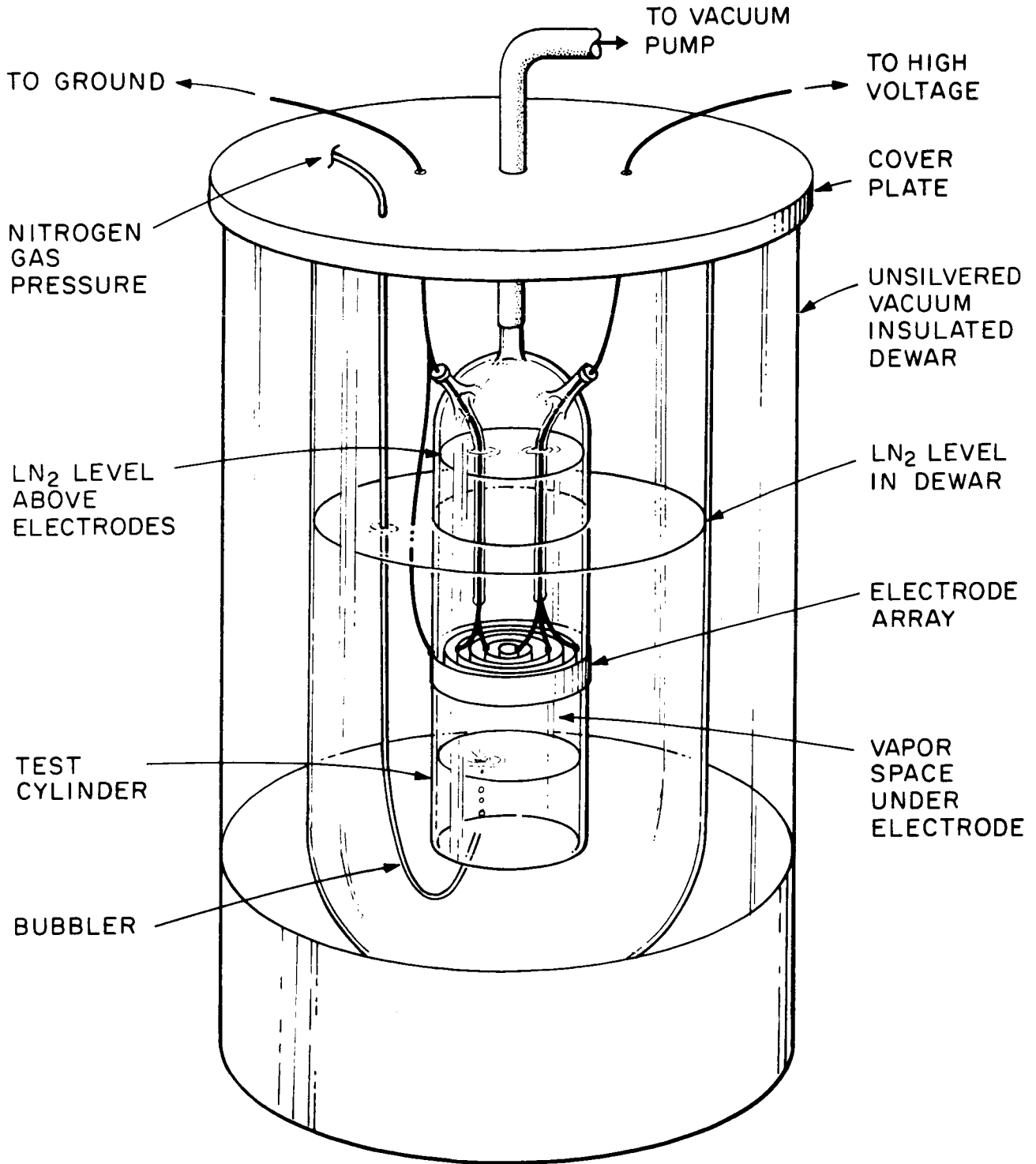
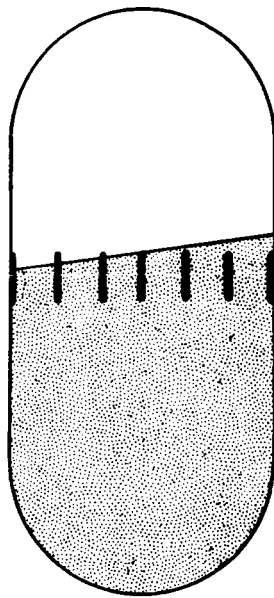
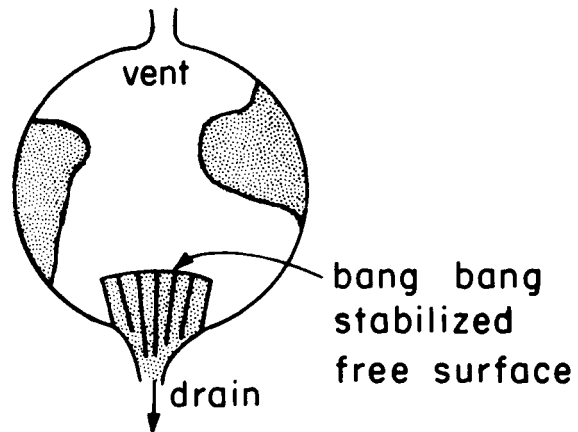


Fig. 12 Experiment to demonstrate bang-bang stabilization of cryogenic liquids. The electrodes are concentric cylinders, as in the apparatus of Fig. 9. The fluid is liquid nitrogen.



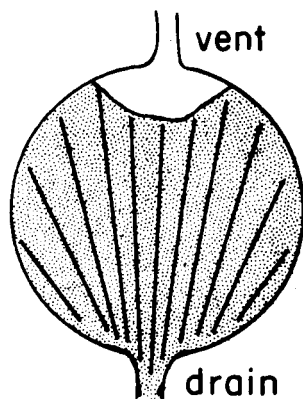
(a)

Sash baffle to avoid amplification at engine cut-off.



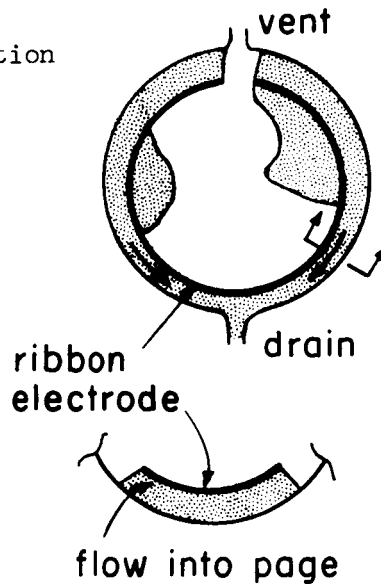
(b)

Partial orientation system to hold liquid at the drain.



(c)

Total orientation system to guarantee liquid at drain and vapor at vent.



(d)

Ribbon electrode for liquid withdrawal through a "wall-less" dielectrophoretic pipe.

Fig. 13 Examples where bang-bang effect is utilized for orientation and sash control. Electrodes are constructed of lightweight screen.

where it displaced the liquid. Thus the upper portion of the tube was filled with liquid nitrogen supported by the pressure of the gas beneath the electrodes, and stabilized by the electrohydrodynamic, bang-bang interaction at the liquid-vapor interface. The voltage was then decreased gradually, until the liquid-vapor interface became unstable and the liquid in the glass column fell. The point of instability with liquid nitrogen was found to be 21.5 kv. Eq. (21) predicts the incipience of instability at 21.2 kv. This agreement is better than would be expected, considering the sources of error involved.

It has been found that, with dc fields, there is an upper limit on the potential required for stable orientation of liquid freon as well as a lower limit. As the voltage is raised, the interface is observed to become overstable, the interfacial oscillations often reaching amplitudes such that the liquid orientation is lost. There are two possible mechanisms for this overstability, both under investigation. One concerns the effects of charge relaxation on interactions at the interface¹⁰ and the second concerns bulk instability of the fluid due to space charge accumulation from a non-ohmic conduction process connected with the generation of carriers at the electrodes.

Applications

Bang-bang stabilization provides an important ingredient in the design of a number of electrohydrodynamic propellant control devices. One obvious application is the slosh baffle shown in Fig. 13a. Analysis indicates that a baffle consisting of concentric cylindrical electrodes one foot high, spaced at two-inch intervals and operating at 100kv, would suppress slosh growth in the S-IV-B LH₂ tank which is anticipated after the booster engine cuts off (and the axial acceleration suddenly decreases from ~ 1 g to 10^{-4} g with a 1 g slosh amplitude of 2 inches).

Another application is in the design of the partial orientation device shown in Fig. 13b. This device positions a small quantity of liquid at the tank sump for engine re-start. Because of the bang-bang stabilization at the free surface, a partial orientation system having a maximum electrode spacing of two inches and operating at 10 kv will withstand adverse accelerations up to $\sim 10^{-3}$ g before the free surface of LH_2 becomes unstable and the liquid drops out.

In the design of total orientation devices of the kind shown in Fig. 13c, it has been found useful to truncate the tops of the electrodes near the vapor vent. This provides bang-bang stabilization for the liquid/vapor interface near the vent, and has been shown in KC-135 flight tests* to be more effective for preventing liquid sloshing into the vent than gradient stabilization alone. For example, a typical total orientation system design for a 40" LOX tank operates at 90 kv with a minimum electrode spacing of one inch and a maximum spacing of 3-1/2 inches. Gradient stabilization will insure the integrity of the liquid/vapor configuration under adverse accelerations up to 4×10^{-4} g, but at the bang-bang stabilized region near the vent, the liquid/vapor interface is stable under adverse accelerations up to 2×10^{-3} g.

The liquid expulsion device in Fig. 13d is a most interesting application of bang-bang stabilization. This lightweight device uses a series of open-sided electrohydrodynamic "pipes" which communicate liquid to the tank drain for zero-g expulsion. Bang-bang stabilization occurs at the free liquid surfaces along the open sides of the "pipes". This liquid can be flowed through these "pipes" until the sum of the frictional and Bernoulli pressure drops exceeds the electrical Maxwell stress at the free surfaces. In a typical

* Conducted under AF Contract No. AF 33(615)-3583

design for a 175,000 lb. LH₂ orbital tanker*, a series of expulsion electrodes is positioned nominally seven inches from the tank wall and operates at 100 kv. This configuration permits stable liquid expulsion at flow rates up to 1000 lbs/min.

* A hemispherically capped cylinder, with 33 foot diameter and a 28 foot cylindrical section.

Appendix

To establish that the dielectrophoretic force should be approximated as shown in Fig. 4a, an analogue experiment was performed. To see the connection between this experiment and Fig. 2, consider the two regions of fluid between the symmetry ground planes of Fig. 14a. Although the symmetry ground planes are imaginary surfaces in the actual bang-bang apparatus, they can be simulated by real metal electrodes, as shown in Fig. 14b. Two channels are so used that fluid is conserved as it is in an actual slosh.

We have already argued that for such a mode, the average dielectrophoretic force per unit area on the slosh pendulum has extreme values of zero (for $\xi = 0$) and $\pm \frac{1}{2}(\epsilon - \epsilon_0)E_0^2$ (for $|\xi| \gg s$; see Fig. 4). It remains only to determine the shape of the curve between these two values. If we assume that the plates have a radius of curvature large enough for the problem to be modeled as two-dimensional, and if the plate height h is sufficiently large, with respect to the plate thickness $d = s/2$, the shape of the $\tau_e(\xi)$ curve can only depend on the two-dimensionless parameters ξ/s and ϵ/ϵ_0 .

We recall that, for a constant potential electric-field system having a capacitance C , dependent on a geometrical displacement ξ , the force is proportional to ¹² $(\partial C / \partial \xi)$. Since we already know the asymptotic value of the average force, it is necessary only to determine the dimensionless curve:

$$\tau_e / \tau_{\max} = \frac{\frac{\partial C}{\partial \xi}}{\left(\frac{\partial C}{\partial \xi} \right)_{\max}}$$

experimentally for the apparatus of Fig. 14b scaled so as to preserve the dimensionless parameters ξ/λ and ϵ/ϵ_0 .

The results of such an experiment are shown in Fig. 15 for two fluids, aroclor ($\epsilon/\epsilon_0 = 5.7$) and corn oil ($\epsilon/\epsilon_0 = 3.1$). It is seen that there is only a

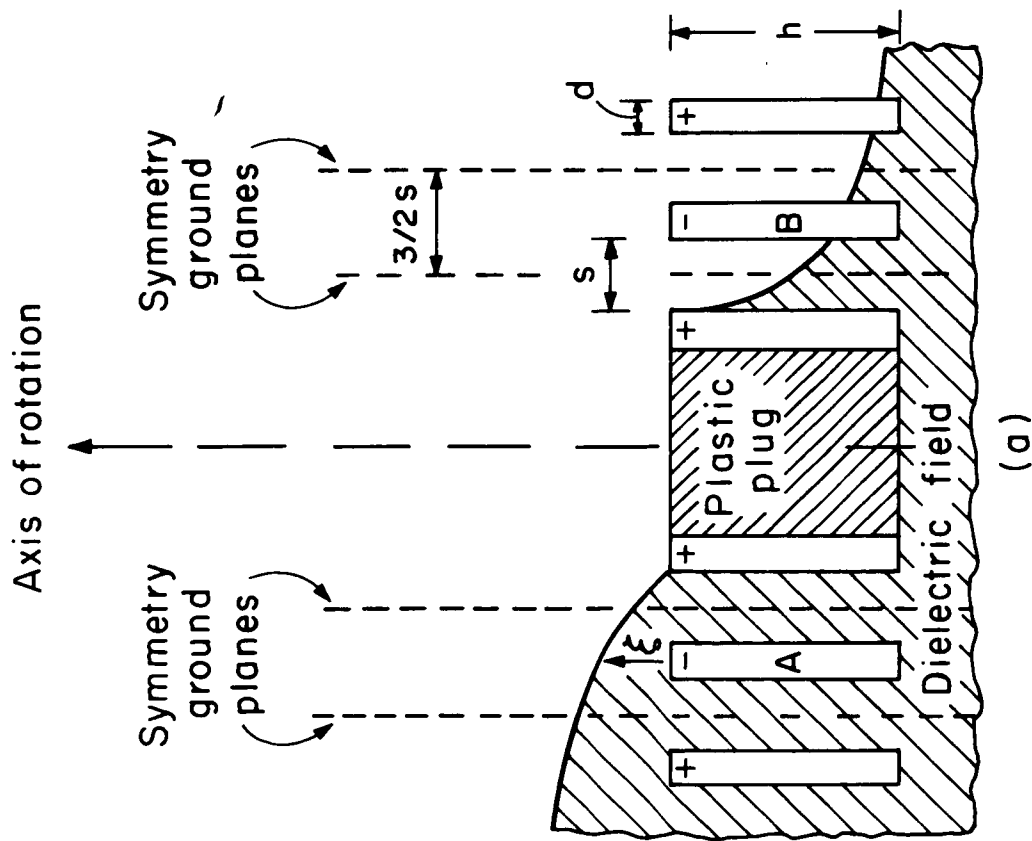
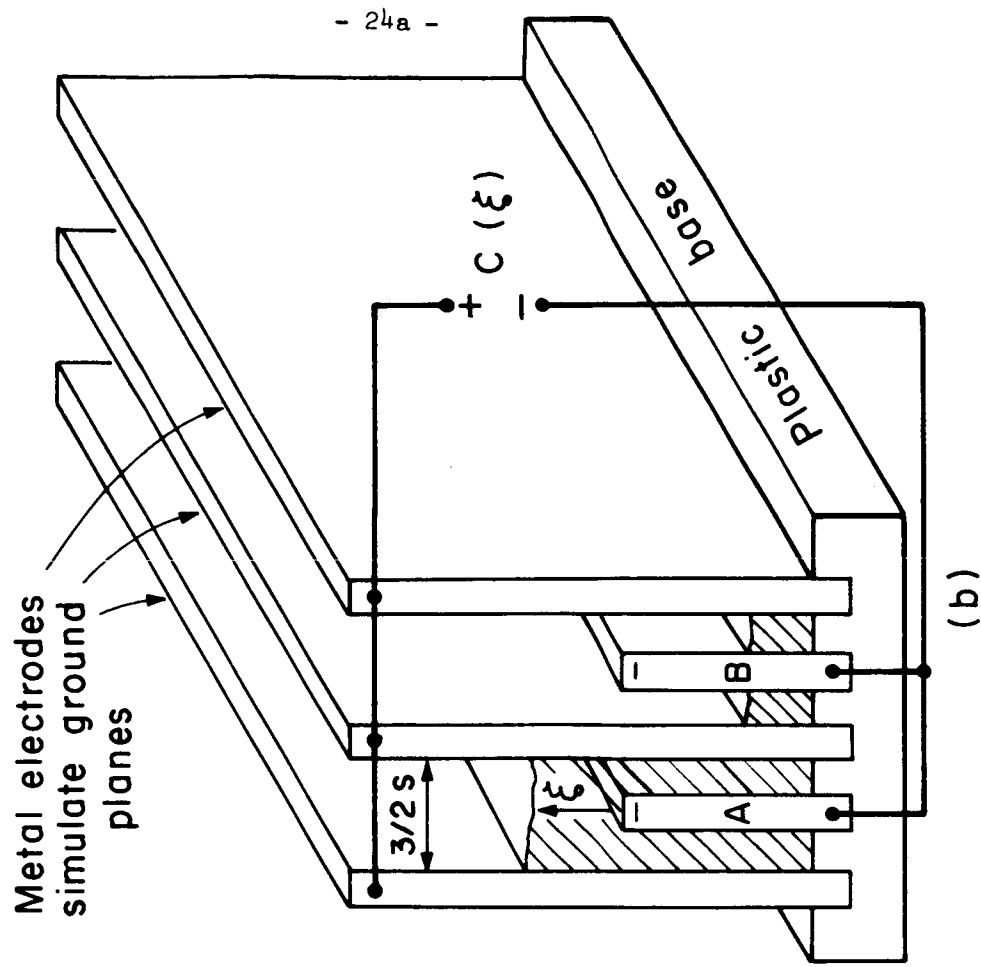


Fig. 14a

Cross-sectional view of electrodes and fluid interface for the geometry of Fig. 2, but with the relative positions of air and liquid reversed



(b)

Analogue apparatus for measuring capacitance as a function of interface deflections

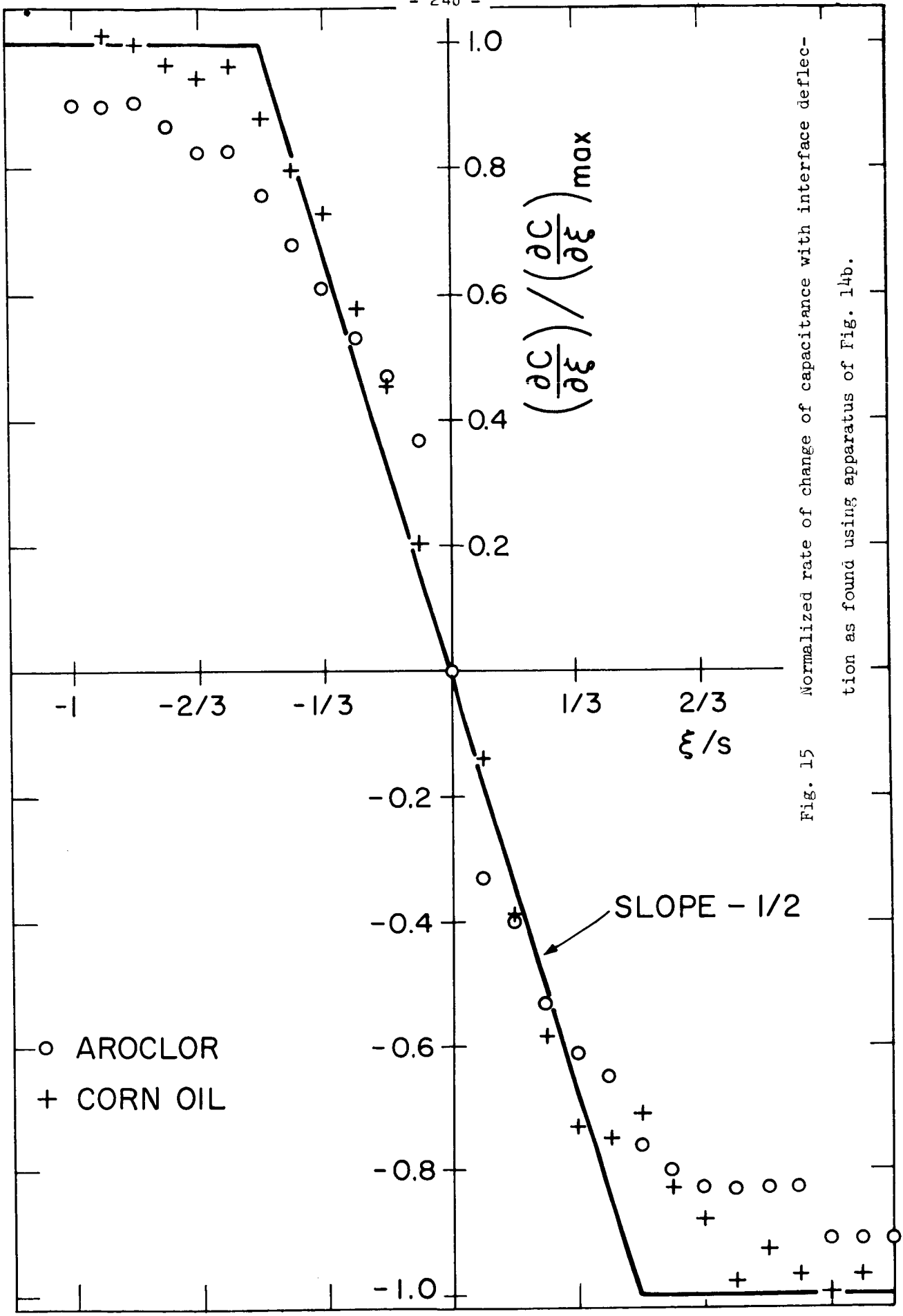


Fig. 15 Normalized rate of change of capacitance with interface deflection as found using apparatus of Fig. 14b.

weak dependence on the factor ϵ/ϵ_0 . The piecewise continuous solid curve is the one used for the pendulum force (see Fig. 4).

Acknowledgments:

This research was sponsored by NASA Grant NsG-368, NASA Contract NAS-8-20553 and Air Force Contract AF33(615)-3583. The authors are indebted to Mrs. Ruth G. Fax and Mr. John R. Blutt for help with portions of the experimental work.

References

1. Gluck, D.F., and Gille, J. P., "Fluid Mechanics of Zero-G Propellant Transfer in Spacecraft Propulsion Systems", ASME Jrl. of Engineering for Industry, Feb. 1965, pp. 1-8.
2. Swalley, F.E., Ward, W.D., and Toole, L.E., "Low Gravity Fluid Behavior and Heat Transfer Results from the S-IVB-203 Flight", Proc. of the Conference on Long-Term Cryo-Propellant Storage in Space, George C. Marshall Space Flight Center, Huntsville, Ala., Oct. 12-13, 1966, pp. 213-232.
3. Barger, J. P., "Method and Apparatus for Orienting Fluids in Zero-Gravity Fields", U.S. Patent No. 3,202,160, Assigned to Dynatech Corp., filed May 24, 1961, issued Aug. 24, 1965.
4. Blackman, J. B., "Dielectrophoretic Propellant Orientation in Zero Gravity", Douglas Paper No. 1292, presented at 7th Symposium on Ballistic Missile and Space Technology, Colorado Springs, Colo., 13-16, Aug. 1962.
5. Reynolds, J.M., Hurwitz, M. et al, "Design Study of a Liquid Oxygen Converter for Use in Weightless Environments", AMRL-TDR-63-42. Contract AF 33(657)-9423, Aerospace Medical Research Labs., Wright-Patterson AFB, Ohio
6. Melcher, J.R., and Hurwitz, M., "Gradient Stabilization of Electrohydrodynamically Oriented Liquids", Jrl. of Spacecrafts & Rockets, 4, (1967), pp. 864-881
7. Stratton, J.R., Electromagnetic Theory, McGraw-Hill Inc., New York, N.Y. 1941, pp. 137-140.

References (continued)

8. Melcher, J.R., Field-Coupled Surface Waves, M.I.T. Press, Cambridge, Mass., 1963, pp. 22-23
9. Reynolds, J.M. and Hurwitz, M. "Electrohydrodynamic Propellant Management Systems for Cryogenic Upper Stages", AIAA Paper 66-922, 1966.
10. Melcher, J. R, and Schwarz, W.F., Jr., "Interfacial Relaxation Overstability in a Tangential Electric Field", M.I.T. Center for Space Research Report CSR-TR-68-2. (1968).
11. Sumner, I.E., "Experimentally Determined Pendulum Analogy of Liquid Sloshing in Spherical and Oblate-Spheroidal Tanks", NASA, Lewis Research Center, TN D-2737, April, 1965.
12. Woodson, H.H. and Melcher, J.R., Electromechanical Dynamics, John Wiley and Sons., Inc., New York, N.Y. 1968, pp. 72-77.